

Figure 1—Plot of  $k_i/b_i$  versus  $\epsilon_i + (a_i/b_i)$  according to Eq. 3. Key: O, chopper-ribbon blender; ●, chopper-ribbon blender followed by an oscillating granulator; ◐, chopper-ribbon blender followed by a rotating granulator; and ◑, fluid bed granulation.

where  $a_i$  and  $b_i$  are constants and the subscript  $i$  refers to the  $i$ th condition (sieve fraction, manufacturing method, or compression pressure). The constants  $a$  and  $b$  are functions of these variables. Therefore, there are 48 lines corresponding to Eq. 1. The correlation coefficients generally were  $>0.94$ , and it is possible to tabulate all 48 values or draw 48 regression lines on one graph. For graphical presentation, a method (10) was used for which the data for each condition were recast in the following form:

$$k/b_i = \epsilon + (a_i/b_i) \quad (\text{Eq. 3})$$

where  $k/b_i$  and  $\epsilon + (a_i/b_i)$  are dimensionless parameters. When one parameter is plotted as a function of the other, a straight line with a unity slope and a zero intercept should result. The 48 data points are plotted in Fig. 1 (the origin is offset), which shows visual agreement with the statements. The treatment is not statistical since the two variables (the left- and right-hand expressions in Eq. 3) are not independent. If a least-squares fit is drawn, the following relationship is obtained:

$$k/b_i = (0.98 \pm 0.05)[\epsilon + (a_i/b_i)] + (0.22 \pm 0.30) \quad (\text{Eq. 4})$$

in accordance with a unity slope and a zero intercept.

Equation 3 includes all of the data points, but Fig. 1 shows that the relationship fails at very low porosity values (high compression pressures). The four cases where  $-a_i/b_i > \epsilon_i$  [i.e., where values of  $\epsilon_i + (a_i/b_i)$  are negative] do not seem to be part of the line. In these four cases, the adherence to Eq. 1 also was marginal (the correlation coefficients for these four points were 0.85–0.91), whereas the agreement was good to excellent in all of the other cases (i.e., correlation coefficients of  $>0.94$ ).

The data and the treatment show that there is a correlation between the dissolution constants,  $k$ , and the porosity,  $\epsilon$ , in the case where a tablet disintegrates into porous granules and the limiting process is the penetration of water into the dislodged granule.

(1) T. Higuchi, R. D. Arnold, S. J. Tucker, and L. W. Busse, *J. Am. Pharm. Assoc., Sci. Ed.*, **41**, 93 (1952).

(2) J. B. Schwartz, *J. Pharm. Sci.*, **63**, 774 (1974).

(3) T. Higuchi, *ibid.*, **52**, 1145 (1963).

(4) J. T. Carstensen, J. L. Wright, K. W. Blessel, and J. Sheridan, *ibid.*, **67**, 48 (1978).

(5) *Ibid.*, **67**, 982 (1978).

(6) J. T. Carstensen, in "Dissolution Technology," L. Leeson and J. T. Carstensen, Eds., APhA Academy of Pharmaceutical Sciences, Washington, D.C., 1974, p. 189.

(7) W. Jost, "Diffusion in Solids, Liquids and Gases," Academic, New York, N.Y., 1952, pp. 45–47.

(8) A. B. Selkirk, *J. Pharm. Pharmacol.*, **25**, 258 (1973).

(9) G. Levy and B. Hayes, *N. Engl. J. Med.*, **262**, 1053 (1960).

(10) J. T. Carstensen, R. Kothari, V. K. Prasad, and J. Sheridan, *J. Pharm. Sci.*, **69**, 290 (1980).

Odile Cruaud  
Dominique Duchêne  
Francis Puisieux  
J. T. Carstensen \*x

Faculte de Pharmacie  
Laboratoire Galenique  
Universite de Paris-Sud  
92290, Chatenay-Malabry, France

Received August 4, 1978.

Accepted for publication December 21, 1979.

\* Sabbatical year. Current address: School of Pharmacy, University of Wisconsin, Madison, WI 53706.

## Identification of Subvisible Barium Sulfate Crystals in Parenteral Solutions

**Keyphrases** □ Barium sulfate—crystal formation in commercial parenteral solutions, identification by polarizing microscopy, scanning electron microscopy, micro X-ray powder diffraction, and micro Raman spectroscopy □ Parenteral solutions, commercial—barium sulfate crystal formation, identification by polarizing microscopy, scanning electron microscopy, micro X-ray powder diffraction, and micro Raman spectroscopy □ Crystals—barium sulfate formation in commercial parenteral solutions, characterization by polarizing microscopy, scanning electron microscopy, micro X-ray powder diffraction, and micro Raman spectroscopy

### To the Editor:

Concern about the presence of particulate matter in parenteral products is increasing, and certain harmful effects when such contamination is introduced into the body during intravenous therapy have been described (1–4). Additionally, studies in our laboratory implicated particulate contamination in infusion fluids as a cause of phlebitis (5–7).

To gain insight into the nature and clinical significance of particulate matter in intravenous solutions, an extensive research program has been undertaken in cooperation with the Food and Drug Administration, which includes the identification of particulate matter in parenteral products. During this investigation, barium sulfate crystals were isolated and identified in six parenteral solutions packaged both in sealed glass ampuls and in glass vials with rubber stoppers. The conclusive identification of barium sulfate crystals was achieved through the correlation of analytical data from polarizing microscopy, scanning electron microscopy with energy-dispersive X-ray analysis capability, micro X-ray powder diffraction, and micro Raman spectroscopy.

With the polarizing microscope, barium sulfate crystals isolated from the parenteral solutions appeared as single or agglomerated, well-formed, birefringent crystals, 8–30

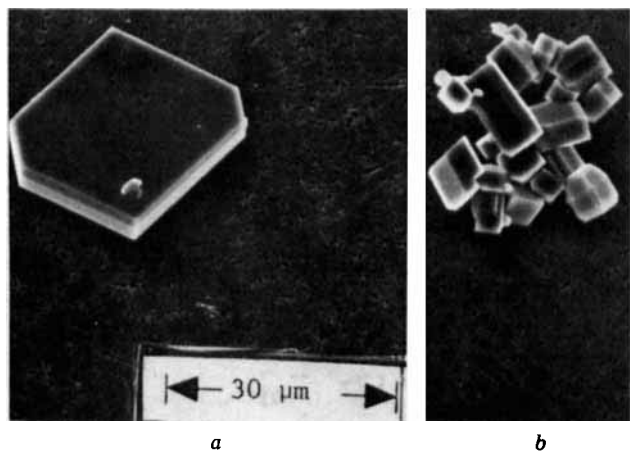


Figure 1—Scanning electron micrographs of barium sulfate crystals isolated from procaine hydrochloride (a) and atropine sulfate (b) (1000X, 20 kv).

μm in maximum linear dimension with symmetrical edges and smooth surfaces. Under crossed polars, the crystals were birefringent and had symmetrical extinction. The high melting point (>300°) is indicative of the inorganic nature of the particles. Following characterization by polarizing microscopy, the crystals were examined by scanning electron microscopy and analyzed by energy-dispersive X-ray analysis to obtain the elemental composition. Under scanning electron microscopy, the crystals appeared as perfect rhombohedra with smooth surfaces (Fig. 1). The energy-dispersive X-ray analysis spectrum (Fig. 2), monitored for 40 sec, indicated strong signals of sulfur (2.31 kev) and barium (4.47, 4.83, 5.13, and 5.45 kev) (8).

To identify the crystals conclusively, micro X-ray powder diffraction was employed. A 57.3-mm diameter X-ray Phillips camera was used with the diameter reduced to 28.98 mm by means of a brass insert, which shortens the exposure time and reduces the dark film background (9). Eight to 10 crystals were subjected to X-rays under vacuum for 12–16 hr. By adjusting the energy output to 35 kv and 15 mamp and using a CuKα radiation source and a nickel filter, a diffraction pattern was obtained. The *d* spacings calculated from the diffraction pattern using the

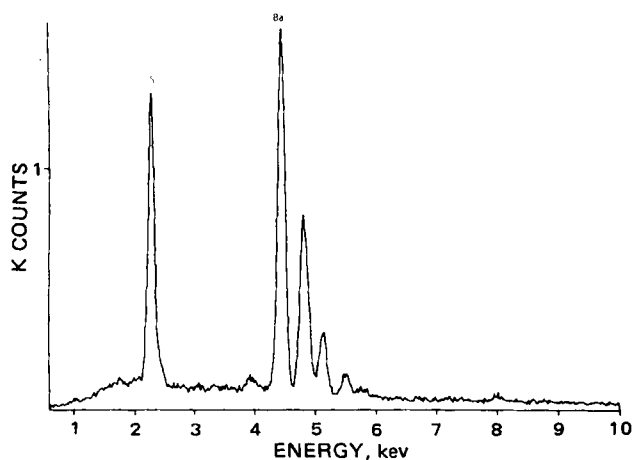


Figure 2—Energy-dispersive X-ray analysis spectrum (40 sec) of barium sulfate crystals from a parenteral solution showing a sulfur signal at 2.3 kev and barium signals at 4.5, 4.8, 5.1, and 5.5 kev.

Table I—Comparison of *d* Spacings of Particles from a Commercial Product with Reported Values for Barium Sulfate<sup>a</sup>

<i>d</i> Spacing for Sample Particles	Reported <i>d</i> Spacing for Barium Sulfate
3.864 (50)	3.900 (57)
3.559 (10)	3.576 (31)
3.424 (100)	3.442 (100)
3.300 (50)	3.317 (67)
3.077 (100)	3.101 (97)
2.812 (50)	2.834 (50)
2.710 (50)	2.726 (47)
2.466 (10)	2.444 (2)
2.319 (10)	2.303 (6)
2.210 (10)	2.209 (27)
2.111 (100)	2.120 (80)
2.056 (10)	2.056 (23)
1.865 (10)	1.857 (16)

<sup>a</sup> The values in parentheses indicate the percent relative intensity of diffraction lines corresponding to various *d* spacings.

Table II—Parenteral Solutions Containing Barium Sulfate Crystals

Product	Type of Glass Container	Source of Sulfate or Bisulfite Ions
Procaine hydrochloride, 2%	30-ml vial	Antioxidant
Kanamycin sulfate, 0.5 g/2 ml	2-ml vial	Drug
Meperidine hydrochloride, 100 mg/ml	1-ml vial	Antioxidant
Magnesium sulfate, 5 g/10 ml	10-ml vial (plunger) and rubber closure	Drug
Atropine sulfate, 0.5 mg/ml	1-ml ampul	Drug
Promethazine hydrochloride, 25 mg/ml	1-ml ampul	Antioxidant

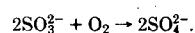
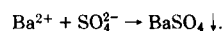
Bragg equation show maximum relative intensities at 3.42, 3.08, and 2.11 Å, which match well with those reported for barium sulfate (10) (Table I).

Barium sulfate crystals in parenteral solutions also were identified by micro Raman spectroscopy<sup>1</sup>. An instrument for this technique became available recently and provides the composition of the particulate sample on the molecular scale. The sample is mounted on an ordinary microscope slide, the laser beam is focused on the crystal to be analyzed, and a Raman spectrum is obtained. The spectrum of particles isolated from a parenteral product (Fig. 3) compares well with the reference spectrum of known barium sulfate crystals (Fig. 4). The spectrum of sample particles exhibited peaks at 455, 988, and 1135 cm<sup>-1</sup>, and the reference particles exhibited peaks at 450, 988, and 1135 cm<sup>-1</sup>.

Using the described microanalytical techniques, crystals detected in six commercial parenteral solutions were identified as barium sulfate. The solutions are listed in Table II; on the basis that barium sulfate forms *in situ*<sup>2</sup>, the sulfate ions appear to originate from the anion of the drug and/or the bisulfite ion of the antioxidant. The barium ions appear to come from the borosilicate glass, which contains up to 5% BaO (11).

<sup>1</sup> Microprobe MOLE, Instruments SA, Metuchen, NJ 08840.

<sup>2</sup> BaO + H<sub>2</sub>O → Ba(OH)<sub>2</sub>.



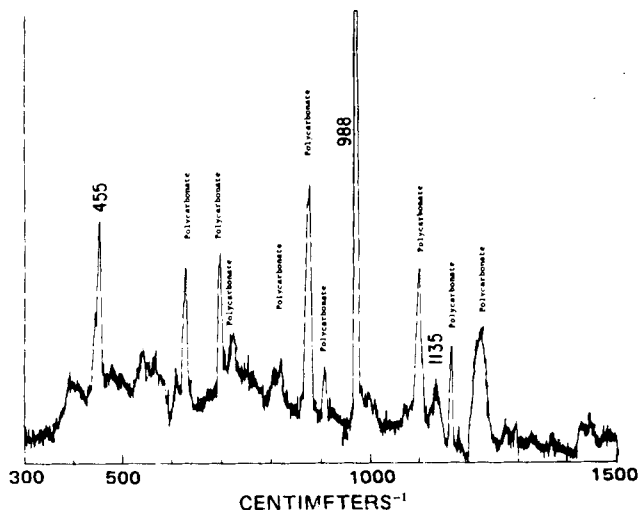


**Figure 3**—Raman spectrum of barium sulfate crystal isolated from a parenteral product on a 0.45- $\mu\text{m}$  polycarbonate filter (Nuclepore Corp., Pleasanton, Calif.). Peaks due to the crystal appear at 455, 988, and 1135  $\text{cm}^{-1}$ .

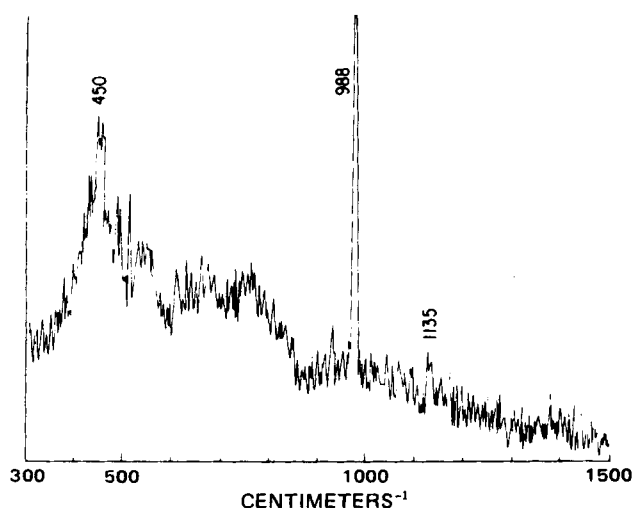


**Figure 4**—Raman spectrum of reference barium sulfate crystals on a glass slide showing peaks at 450, 988, and 1135  $\text{cm}^{-1}$ .

In a preliminary experiment, we were able to generate barium sulfate crystals in 10-ml ampuls containing particulate-free solutions of either 0.2% sodium sulfate or 0.2% sodium bisulfite. These ampuls were autoclaved for 2 hr and stored at room temperature for 30 days. Ampuls containing particulate-free water treated identically did not produce any crystals.

Barium sulfate is so insoluble that it can be tolerated orally since it is the barium ion that is highly toxic. However, crystals injected intravenously will lodge in various tissues, depending on their size, and can cause irritation. Therefore, it is important to define the conditions under which barium sulfate crystals form in parenteral products and to devise a means for preventing their formation, such as siliconizing the glass surface or adding either a complexing agent (*i.e.*, ethylenediaminetetraacetic acid) or a nucleation inhibitor (*i.e.*, polyvinylpyrrolidone).

- (1) E. J. Bruning, *Virchows Arch.*, **327**, 460 (1955).
- (2) S. Sarrut and C. Nezelof, *Presse Med.*, **68**, 375 (1960).
- (3) J. M. Garvan and B. W. Gunner, *Med. J. Aust.*, **2**, 140 (1963).

- (4) *Ibid.*, **2**, 1 (1964).
- (5) P. P. DeLuca, R. Rapp, B. Bivins, H. McKean, and W. Griffen, *Am. J. Hosp. Pharm.*, **32**, 1001 (1975).
- (6) H. G. Schroeder and P. P. DeLuca, *ibid.*, **33**, 543 (1976).
- (7) S. Rusmin, R. Rapp, B. Bivins, and P. P. DeLuca, *Bull. Parent. Drug Assoc.*, **31**, 1 (1977).
- (8) W. C. McCrone and J. G. Delly, "The Particle Atlas, Edition II," vol. III, Ann Arbor Science Publishers, Ann Arbor, Mich., 1973, p. 747.
- (9) *Ibid.*, pp. 119-129.
- (10) "X-Ray Powder Data File No. 5-0488," ASTM Special Technical Publication 48-J, American Society for Testing and Materials, Philadelphia, Pa., 1960, p. 622.
- (11) S. V. Sanga, *J. Parent. Drug Assoc.*, **33**, 61 (1979).

Sam Boddapati  
L. David Butler  
Sophann Im  
Patrick P. DeLuca<sup>x</sup>  
College of Pharmacy  
University of Kentucky  
Lexington, KY 40506

Received October 9, 1979.

Accepted for publication February 21, 1980.

Supported by FDA Contract 223-77-3001.

## Prediction of Steady-State Behavior of Metabolite from Dosing of Parent Drug

**Keyphrases** □ Metabolism—prediction of steady-state metabolite concentration, cinromide and carbamazepine, monkeys □ Steady-state concentration—prediction of metabolite and parent drug concentrations, metabolism, cinromide and carbamazepine, monkeys □ Cinromide—prediction of steady-state metabolite concentration, monkeys □ Carbamazepine—prediction of steady-state metabolite concentration, monkeys

### To the Editor:

It has become apparent that the metabolites of many drugs contribute to the observed clinical efficacy and/or toxicity (1). In assessing the contribution of a given metabolite during chronic dosing, the relative steady-state concentrations of the metabolite and the parent drug (as well as the relative potencies) must be determined. This steady-state ratio was shown to be dependent only on the formation and elimination clearances of the metabolite (2, 3):

$$\frac{C_m^*}{C_p^*} = \frac{Cl_f}{Cl_m} = \frac{f_m Cl_p}{Cl_m} \quad (\text{Eq. 1})$$

where  $C_m^*$  and  $C_p^*$  represent the steady-state plasma concentrations of the metabolite and the parent drug, respectively;  $Cl_f$  and  $Cl_m$  represent the formation clearance and intrinsic clearance (4) of the metabolite, respectively;  $f_m$  is the fraction of the parent drug metabolized to this metabolite; and  $Cl_p$  is the systemic clearance of the parent drug.

From Eq. 1, it appears that knowledge of the metabolite clearance and the fraction metabolized (or formation clearance) is necessary to calculate this ratio. The purpose of the present report is to show that the steady-state metabolite to parent drug ratio, as well as the actual steady-state metabolite concentration, can be determined from administration of a single dose of the parent drug without administration of the metabolite. A change in the admin-